Conformation and crystal packing sensitivity to substitution of thioxo- and oxo-tetrazane derivatives†

Olivier Oms,* Lucie Norel, Lise-Marie Chamoreau, Hélène Rousselière and Cyrille Train*

Received (in Montpellier, France) 3rd February 2009, Accepted 1st April 2009
First published as an Advance Article on the web 12th May 2009
DOI: 10.1039/b902225b

The synthesis of a series of six thioxo-tetrazane derivatives is reported. The crystal structures of five of these new products and the corresponding oxo-compounds (except the 4,6-dimethylpyrimidyl derivative) including two new crystal structures are also described and compared. The structural data show the importance of the substituent for the intramolecular arrangement while the heteroatom (S, O) does not play any role at this stage: the 2-pyridyl, 4,6-dimethylpyrimidyl and 8-quinolyl groups occupy a pseudo-equatorial position related to the existence of an intramolecular hydrogen bond where the substituent acts as an acceptor. 2-Hydroxyphenyl moieties occupy a pseudo-axial position related to the existence of an intramolecular hydrogen bond where the substituent acts as a donor. In the sole example where an intramolecular hydrogen bond is not present (2-imidazolyl derivatives), the preference for the pseudo-axial conformation is determined by the hyperconjugative effect. In contrast with the intramolecular arrangement, the crystal packing strongly depends on the choice of the heteroatom. It shows noticeable differences related to the variable involvement of C=S and C=O functions as hydrogen-bond acceptors and the occurrence of π stacking between the molecules. It thus appears that the sulfur atom of the thioxotetrazanes is always involved in hydrogen bonding whereas this is not the case for the oxygen atom of the oxotetrazane analogues. This result contrasts with the statistical treatment of the crystal structures of the Cambridge Structural Database in the urea/thiourea series and could be related to the steric hindrance imposed by the two methyl groups borne by the nitrogen atoms located in the α positions of the C=X function (X = S, O).

Introduction

The synthesis of molecular materials fully exploits the whole range of interactions from strong intramolecular to weaker intermolecular ones.[1] Among the latter, hydrogen bonds are the most reliable for crystal engineering because of their geometrical constraints and intensities. For every family of compounds, the anticipation of the crystal packing of forthcoming compounds relies on the description and understanding of the crystal structures of as many members of the family as possible.[2] In this respect the urea and, to a lesser extent, thiourea derivatives (Scheme 1) is a case study. They have been widely studied because they are synthetically versatile and able to develop rich hydrogen-bond patterns that have been used to form superstructures with various topologies or to design anion binding groups.[3] The hydrogen bonds exploit the accepting ability of the O or S heteroatom and the donating ability of the nitrogen atoms.

By displacing the hydrogen-bond donors and modifying the electronic delocalisation involving the nitrogen atoms and the heteroatom, the study of tetrazane containing derivatives (Scheme 1) appear as a natural extension of the study of the (thio)ureas. The versatility of their chemistry[4–9] allows varying the heteroatom as well as the substituent almost at will. Nevertheless, up to date, this family of molecules has mainly been used as a precursor of verdazyl radicals, promising species in molecular magnetism,[10–14] and little is known about their organisation in the solid state.[9,15]

We report herein the synthesis of six original compounds, mainly thione derivatives. We present seven novel crystal structures of tetrazane-based derivatives and compare the conformation of the molecules and the crystal packing of nine of such compounds by analysing the nature of the interactions

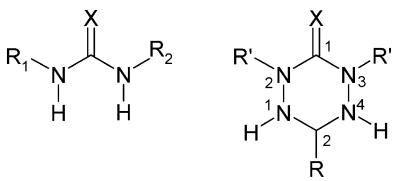

Scheme 1 (Thio)urea- (left) and (thio)oxotetrazane- (right) based molecules (with crystallographic numbering scheme).

"Matériaux Magnétiques Moléculaires et Absorption X" et "Centre de Résolution de Structures", Institut Parisien de Chimie Moléculaire, UMR CNRS 7201UPMC-Univ. Paris 06, case 42, 4 place Jussieu, F-75252, Paris cedex 05

† CCDC reference numbers 714410 (**1b**), 714408 (**1c**), 714409(**1e**), 714411(**1f**), 714425 (**1g**), 714424 (**2f**) and 714423 (**2g**). For crystallographic data in CIF or other electronic format see DOI: 10.1039/b902225b

(hydrogen bonds, π stacking) and the influence of the R substituent and X heteroatom.

Results

Synthesis

The synthesis of the 1,5-dimethyl-3-R-6-thioxo-1,2,4,5-tetrazanes **1b–g** (**b**: R = 2-imidazolyl, **c**: R = 2-pyridyl, **d**: R = carboxylic acid, **e**: R = 4,6-dimethylpyrimidyl, **f**: R = 8-quinolyl, **g**: R = 2-hydroxyphenyl) and the corresponding oxo derivatives **2b–g** follows the synthetic pathway described by Neugebauer[4] with minor modifications. 2,4-Dimethylthiocarbonohydrazide (**1a**) and 2,4-dimethyl carbonohydrazide (**2a**) are prepared by the reaction of methylhydrazine with thiophosgene or triphosgene, respectively. In a second step, the condensation of **1a** or **2a** with selected aldehydes leads to the desired products. While **2b–e** and **2g** have been already reported,[4,7,12,15] only **1b** is mentioned in the literature[16] for the thioxo series and, in this case, no further data were presented. The synthesis of six new sulfur-substituted derivatives thus demonstrates the versatility of the synthetic scheme proposed by Neugebauer while the obtained yields demonstrate its efficiency (Scheme 2). We notice better results for the oxo derivatives (yield range: 65–100%) than for the thioxo ones (51–75%). Following the conditions described for the preparation of the 4-pyridyl derivative,[4] **1c** was obtained in low yield (20%, room temperature). Working in refluxing methanol leads to an improvement of the reaction yield (44%). **1g** and **2g** are the only compounds that must be synthesized at room temperature. In the first case, the crude product of the reaction is a mixture of **1g** with a diimine formed by the reaction of one molecule of **1a** and two molecules of salicylaldehyde. High temperatures favor the formation of the diimine. By working at room temperature using a slight excess of **1a**, we obtained 91% of **1g** and 9% of the by-product (estimated by ^{1}H NMR). The higher solubility of the diimine in chloroform allows the isolation of **1g** in relatively good yield (60%). Similarly, **2g** is a minor product when the reaction occurs in refluxing methanol (19% estimated by ^{1}H NMR) whereas the reaction is more efficient at room temperature with an excess of **2a** (yield: 69%). In this case, the purification consists of triturating the residue with ethyl acetate to eliminate the diimine by-product.

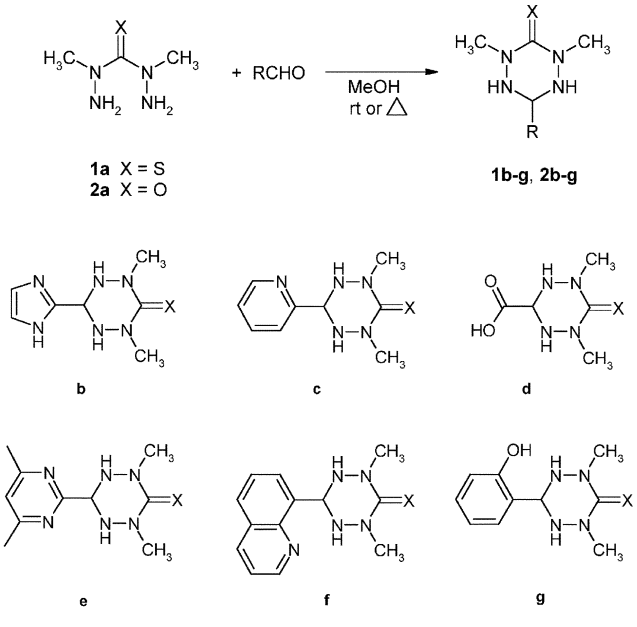

Yield	1b 58%	1c 44%	1d 75%	1e 71%	1f 51%	1g 60%
	2b 74%	2c 65%	2d 100%	2e 86%	2f 67%	2g 69%

Scheme 2 Synthesis of tetrazanes.

Crystal structure analysis

The structures of **2b** and **2c** were previously described[12,15] while no structural data were obtained for **1d**, **2d** and **2e**. We report here the crystal structures of seven compounds (**1b–g**, **2f–g**) whose crystallographic parameters are summarized in Table 1.

In all these structures, the tetrazane rings present an overall similar arrangement: N2 and N3 have essentially planar geometries while N1 and N4 adopt pyramidal ones (Scheme 1). Opposite to the sp^2-hybridized C1 atom, C2 presents a tetrahedral environment related to its sp^3-hybridization. The bond lengths of the tetrazane rings are given in Table 2. To go beyond these general features, we will examine the specificities of the seven new structures reported here.

1,5-Dimethyl-3-(2′-imidazolyl)-6-thioxo-1,2,4,5-tetrazane 1b

The molecular structure of **1b** is shown in Fig. 1. C2 is 0.652 Å away from the average plane constituted by the five other atoms of the tetrazane ring. The imidazole group occupies a pseudo-axial position and the dihedral angle between the average planes of imidazole and tetrazane ring is 87.03(10)°. The crystal packing is governed by hydrogen bonds (Fig. 2) between: (i) the nitrogen atom and the NH group of the imidazole substituent, (ii) the sulfur atom and the NH group of the tetrazane moiety. In the former case, the non-protonated nitrogen atom of imidazole acts as a hydrogen-bond acceptor and the NH group acts as a hydrogen-bond donor leading to chains along the *b*-axis (N5···N6, 2.993(2) Å, N6···H–N5 angle, 176°). In the latter, the C=S function is involved in two bifurcated hydrogen bonds with N1H (S···N1, 3.487(2) Å; S···H–N1 angle, 149°) and N4H (S···N4, 3.437(2) Å; S···H–N4 angle, 150°) forming of zigzag chains of aligned molecules along the *c*-axis. Two neighbouring rows are running in opposite directions. Altogether, hydrogen bonds lead to the formation of two-dimensional arrays of molecules.

1,5-Dimethyl-3-(2′-pyridyl)-6-thioxo-1,2,4,5-tetrazane 1c

The molecular structure of **1c** is shown in Fig. 3. The distance between C2 and the average plane constituted by the five other atoms of the tetrazane ring is 0.582 Å. The pyridine moiety linked to the C2 atom occupies a pseudo-equatorial position and the dihedral angle between the average planes of pyridine and tetrazane ring is 77.85(13)°. The nitrogen atom of the pyridine group is directed towards the axial hydrogen atom

Table 1 Crystallographic data for the tetrazane derivatives

Formula	**1b** $C_7H_{12}N_6S$	**1c** $C_9H_{13}N_5S$	**1e** $C_{10}H_{16}N_6S$	**1f** $C_{13}H_{15}N_5S$	**1g** $C_{10}H_{14}N_4OS$	**2f** $C_{13}H_{15}N_5O$	**2g** $C_{10}H_{14}N_4O_2$
M_r	212.29	223.30	252.35	273.36	238.31	257.30	222.25
T/K	250(2)	200(2)	200(2)	200(2)	200(2)	200(2)	200(2)
System	Monoclinic	Monoclinic	Triclinic	Monoclinic	Monoclinic	Monoclinic	Monoclinic
Space group	$P2_1/c$	$P2_1/c$	$P\bar{1}$	$P2_1/c$	$P2_1/c$	$P2_1/c$	Cc
a/Å	9.8198(12)	11.9056(17)	7.6762(13)	12.1254(10)	5.6910(5)	7.8076(7)	5.3123(8)
b/Å	9.615(2)	9.6629(7)	8.5120(12)	14.916(2)	18.042(2)	15.593(2)	23.048(3)
c/Å	10.898(3)	11.3482(19)	10.3122(12)	15.9171(19)	11.6058(12)	10.9987(14)	9.1244(14)
α/°	90	90	104.177(10)	90	90	90	90
β/°	92.127(17)	118.320(9)	102.599(11)	108.354(8)	101.178(11)	107.222(10)	103.276(13)
γ/°	90	90	93.444(13)	90	90	90	90
V/Å^3	1028.2(4)	1149.3(3)	632.94(16)	2732.4(6)	1169.0(2)	1279.0(3)	1087.3(3)
Z	4	4	2	8	4	4	4
D_c/g cm^3	1.371	1.291	1.324	1.329	1.354	1.336	1.358
μMo-Kα)/mm^{-1}	0.287	0.258	0.245	0.231	0.262	0.090	0.098
F(000)	448	472	268	1152	504	544	472
θ range/°	2.83–30.00	2.87–30.01	2.10–32.00	1.77–30.01	2.88–30.00	3.03– 30.00	3.54–29.99
Refl. coll./indep./obs.	7533/2963/1669	16 000/3352/2162	17386/4321/2711	18467/7840/2881	14544/3396/2199	15171/3699/2154	5680/1584/1096
R(int)	0.0577	0.0477	0.0532	0.0807	0.0664	0.0573	0.0479
No. variables	129	136	158	343	148	175	147
Gof on F^2	0.995	1.086	1.018	0.911	1.005	1.030	1.036
$R1$ ($I > 2\sigma(I)$)	0.0543	0.0621	0.0483	0.0552	0.0451	0.0511	0.0459
$wR2$ (all data)	0.1399	0.2046	0.1334	0.1632	0.1226	0.1404	0.1086

Table 2 Bond lengths (Å) for the tetrazane core

	C1–N2	C1–N3	N2–N1	N3–N4	N1–C2	N4–C2
1b	1.361(3)	1.356(3)	1.438(2)	1.443(2)	1.467(3)	1.468(2)
1c	1.359(3)	1.354(3)	1.431(3)	1.439(3)	1.451(3)	1.441(3)
1e	1.365(2)	1.368(2)	1.440(2)	1.439(2)	1.475(2)	1.478(2)
1f (1)	1.357(4)	1.351(4)	1.455(3)	1.444(3)	1.473(3)	1.470(3)
1f (2)[a]	1.356(4)	1.354(4)	1.445(3)	1.447(3)	1.469(3)	1.480(3)
1g	1.358(2)	1.353(2)	1.435(2)	1.439(2)	1.490(2)	1.456(2)
2f	1.370(2)	1.371(2)	1.445(2)	1.435(2)	1.472(2)	1.465(2)
2g	1.373(3)	1.368(3)	1.443(3)	1.448(3)	1.477(3)	1.465(4)

[a] Values related to the second tetrazane ring of **1f**: C14–N8, C14–N7, N8–N9, N7–N6, N9–C15 and N6–C15, respectively.

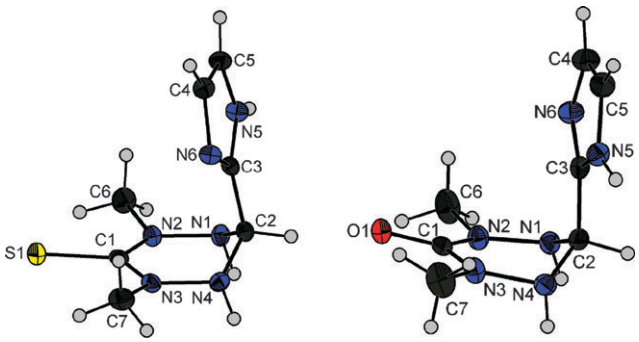

Fig. 1 Structures of **1b** (left) and **2b** (right, adapted from ref. 12). Thermal ellipsoids drawn at 30% probability level.

HN4 constituting an intramolecular hydrogen bond (N5···N4, 2.833(3) Å, N5···H–N4 angle, 108°) leading to the formation of a five-membered ring. Intermolecular hydrogen bonding is also observed (Fig. 4). Two neighboring molecules are connected to one another by two hydrogen bonds involving the C=S function and one NH group (S···N1, 3.529(2) Å; S···H–N1 angle, 161°) leading to the formation of dimers.

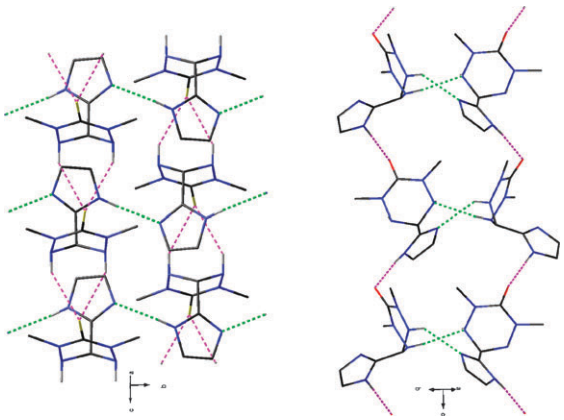

Fig. 2 Intermolecular interactions in **1b** (left) and **2b** (right) (dashed pink line: C=X···HN, dashed green line: N···HN hydrogen bonds). Hydrogen atoms of C–H groups are omitted for clarity.

1,5-Dimethyl-3-(4′,6′-dimethylpyrimidyl)-6-thioxo-1,2,4,5-tetrazane 1e

The molecular structure and the crystal packing of **1e** are shown in Fig. 5. C2 is 0.620 Å from the average plane of the tetrazane ring. The pyrimidyl substituent occupies a pseudo-equatorial position and the dihedral angle is 88.09(7)°. One nitrogen atom of the pyrimidine substituent is involved in two intramolecular hydrogen bonds with N1H (N5···N1, 2.841(2) Å, N5···H–N1 angle, 104°) and N4H (N5···N4, 2.855(2) Å, N5···H–N4 angle, 109°). The C=S group participates to two bifurcated intermolecular hydrogen bonds with N1H (S···N1, 3.603(2) Å; S···H–N1 angle, 145°) and N4H (S···N4, 3.570(1) Å; S···H–N4 angle, 146°) of the tetrazane ring. A distance of 3.416 Å, associated with π–π interactions, separates the average planes of the pyrimidine rings leading to the formation of staggered dimers along the b axis. The combination of these two types of intermolecular interactions leads to the formation of mixed supramolecular chains.

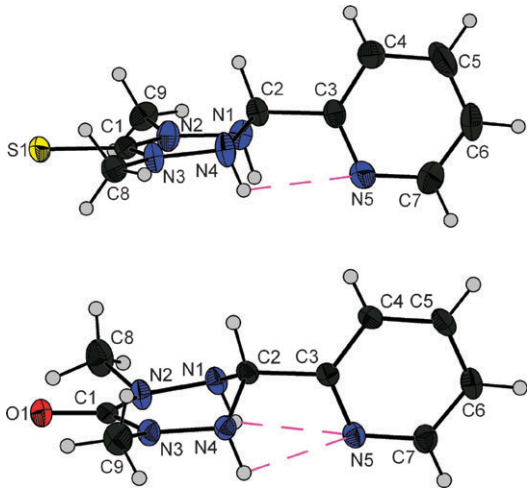

Fig. 3 Structures of **1c** (top) and **2c** (below) (dashed purple line: intramolecular interactions). Thermal ellipsoids drawn at 30% probability level.

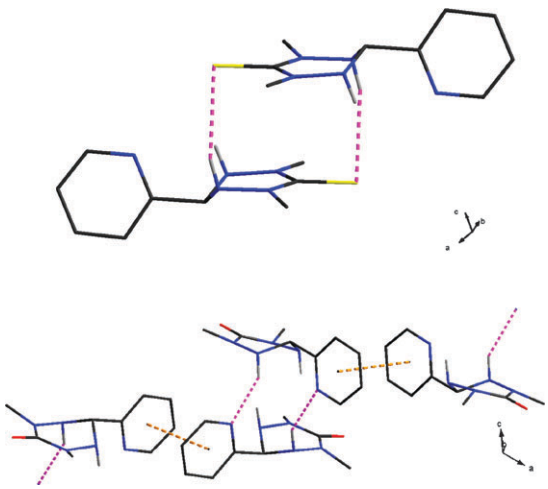

Fig. 4 Intermolecular interactions in **1c** (top) and **2c** (below) (dashed pink line: hydrogen bonds, dashed gold line: π stacking). Hydrogen atoms of C–H groups are omitted for clarity.

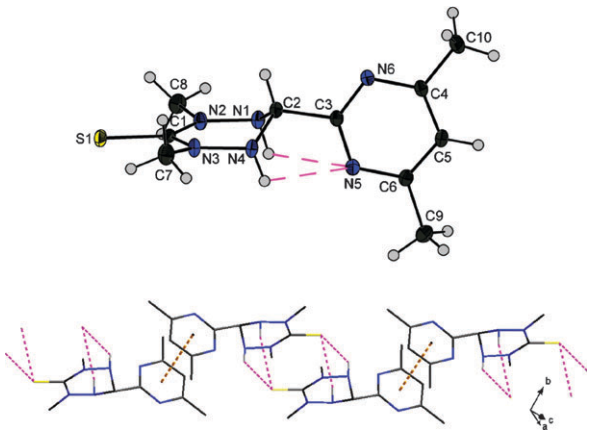

Fig. 5 Structure (top, dashed purple line: intramolecular interactions, thermal ellipsoids drawn at 30% probability level) and intermolecular interactions (below, dashed pink line: C═S···HN hydrogen bonds, dashed gold line: π stacking) of **1e**.

1,5-Dimethyl-3-(8′-quinolyl)-6-thioxo-1,2,4,5-tetrazane 1f

Two molecules are present in the asymmetric unit (Fig. 6). For the S1-containing molecule, the quinolyl substituent occupies a pseudo-equatorial position and is almost perpendicular to the tetrazane ring (dihedral angle: 87.88(11)°). An intramolecular hydrogen bonding is observed (N5···N4, 2.953(3) Å, N5···H–N4 angle, 130°; N5···N1, 3.030(3) Å, N5···H–N1 angle, 118°). For the S2-containing molecule, the quinolyl substituent also occupies a pseudo-equatorial position with a dihedral angle of 85.15(11)° and it is involved in intramolecular hydrogen bonding (N6···N10, 2.923(3) Å, N10···H–N6 angle, 124°; N9···N10, 3.101(3) Å, N10···H–N9 angle, 123°) as well. In the overall structure (Fig. 7), only one weak intermolecular hydrogen bond is observed involving the C═S function and a NH group (S1···N9, 3.628(2) Å; S1···H–N9 angle, 151°). Concerning the quinoline moieties along the *b* axis, the measured distances between the centroids of the four cycles range from 3.955(2) to 5.101(2) Å. Although the minimum angle between close quinoline planes is relatively high (6.93(8)°), these values can be associated with π–π interactions leading to the formation of infinite stacks along the *b*-axis.[17] The hydrogen bonds between these stacks lead to the formation of mixed supramolecular two dimensional brick-wall features.

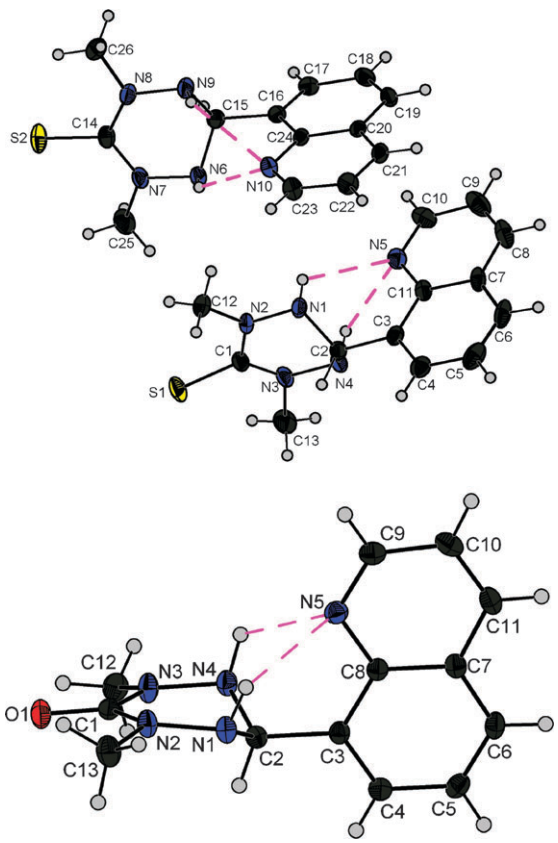

Fig. 6 Structures of **1f** (top) and **2f** (below) (dashed purple line: intramolecular interactions). Thermal ellipsoids drawn at 30% probability level.

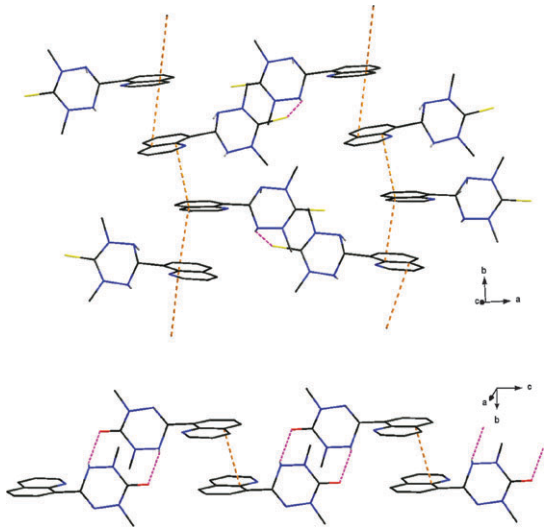

Fig. 7 Intermolecular interactions in **1f** (top) and **2f** (below) (dashed pink line: C═X···HN hydrogen bonds, dashed gold line: π stacking). Hydrogen atoms of C–H groups are omitted for clarity.

1,5-Dimethyl-3-(8′-quinolyl)-6-oxo-1,2,4,5-tetrazane 2f

In this compound (Fig. 6), the distance from the average plane of the tetrazane ring to C2 is 0.617 Å. The quinolyl substituent occupies a pseudo-equatorial position leading to two intramolecular hydrogen bonds (N5···N1, 2.956(2) Å, N5···H–N1 angle, 129°; N5···N4, 3.087(2) Å, N5···H–N4 angle, 124°). The dihedral angle formed with the tetrazane average plane is 84.55(6)°. π-Stacking between quinoline moieties is observed in the overall structure (Fig. 7) characterized by an inter-planar distance of 3.601 Å leading to the formation of staggered dimers along the *b*-axis. Moreover, one weak intermolecular hydrogen bond involves the oxygen atom and a NH group of a neighboring molecule (O1···N4, 3.383(2) Å, O1···H–N4 angle, 142°) forming hydrogen-bonded dimers. The combination of these two types of intermolecular interactions leads to the formation of mixed supramolecular chains running along the *c*-axis.

1,5-Dimethyl-3-(2′-hydroxyphenyl)-6-thioxo-1,2,4,5-tetrazane 1g

The molecular structure of **1g** is shown in Fig. 8. C2 is 0.658 Å away from the average plane constituted by the five other atoms of the tetrazane ring. The hydroxyphenyl group occupies a pseudo-axial position and the dihedral angle between the average planes of the two rings is 86.05(8)°. We observe an intramolecular hydrogen bond involving the hydroxyl group (O1···N1, 2.722(2) Å, N1···H–O1 angle, 150°). In the crystal packing (Fig. 9), two bifurcated hydrogen bonds involving the C═S function and two NH groups (S1···N1, 3.576(2) Å, S1···H–N1 angle, 154°; S1···N4, 3.371(2) Å, S1···H–N4 angle, 154°) lead to the formation of chains along the a-axis.

1,5-Dimethyl-3-(2′-hydroxyphenyl)-6-oxo-1,2,4,5-tetrazane 2g

The molecular structure of **2g** is shown in Fig. 8. C2 is 0.688 Å far from the average plane of the tetrazane ring. The 2-hydroxyphenyl substituent occupies a pseudo-axial position and the OH group is involved in an intramolecular hydrogen bond (O2···N1, 2.716(3) Å, N1···H–O2 angle, 147°). The dihedral angle between the average planes of the tetrazane ring and the 2-hydroxyphenyl moiety is 85.82(13)°. The crystal packing (Fig. 9) reveals two bifurcated hydrogen bonds involving the carbonyl group and two NH functions of the neighboring molecule (O1···N1, 3.024(3) Å, O1···H–N1 angle, 145°; O1···N4, 3.052(3) Å, O1···H–N4 angle, 151°) leading to the formation of chains along the *a*-axis.

Discussion

The analysis of the crystal structures of thioxo- and oxo-tetrazanes allows to delineate the influence of the R substituent as well as of the heteroatom on both the intra- and the inter-molecular organization of the tetrazane molecules.

As far as intramolecular arrangement is concerned (data for intramolecular hydrogen bonds are summarized in Table 3), two situations have been encountered: the R substituent can be either in pseudo-equatorial (pyridyl, pyrimidyl and quinolyl)

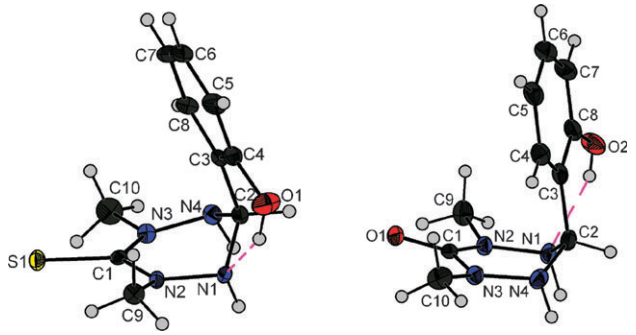

Fig. 8 Structures of **1g** (left) and **2g** (right) (dashed purple line: intramolecular interactions). Thermal ellipsoids drawn at 30% probability level.

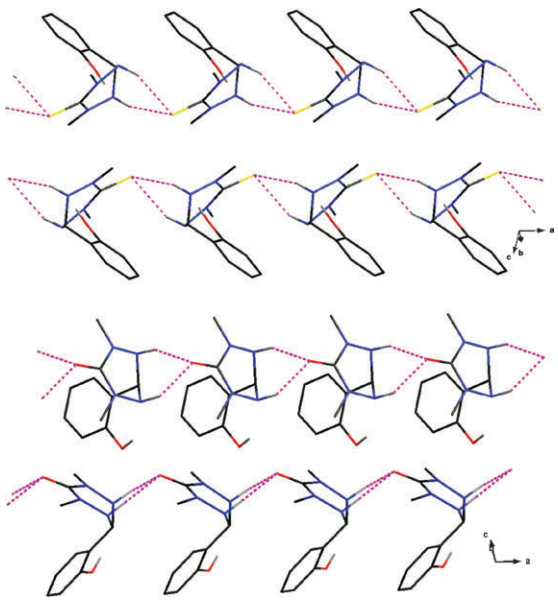

Fig. 9 Intermolecular interactions in **1g** (top) and **2g** (below) (dashed pink line: C═X···HN hydrogen bonds). Hydrogen atoms of C–H groups are omitted for clarity.

Table 3 Intramolecular hydrogen bonds

		DH···A distance (Å)	DH···A angle (°)
1c	N4H···N5	2.44	108
1e	N4H···N5	2.43	109
	N1H···N5	2.47	104
1f	N4H···N5	2.32	130
	N1H···N5	2.53	118
	N6H···N10	2.34	124
	N9H···N10	2.53	123
2f	N4H···N5	2.42	124
	N1H···N5	2.26	129
1g	O1H···N1	1.86	150
2g	O2H···N1	2.07	147

or pseudo-axial (imidazolyl, hydroxyphenyl) positions. This is actually independent of the heteroatom and fully determined by the R substituent. By scrutinizing the intramolecular interactions encountered when the compounds adopt a pseudo-equatorial position, it appears that in all cases this conformation is linked with the existence of an intramolecular hydrogen bond between the substituent, whose heteroatom acts as an acceptor and the N1–H and/or N4–H groups of the tetrazane ring, acting as donors (Table 3). The importance of intramolecular hydrogen bonding also holds for the hydroxyphenyl substituted derivatives **1g** and **2g**. Nevertheless, in these cases, the pseudo-axial conformation is favored because it allows the formation of a hydrogen bond between the substituent acting as a donor and the N1 atom of the tetrazane ring acting as an acceptor. The imidazole substituted derivatives **1b** and **2b** (Fig. 1) deserve additional inspection since no intramolecular hydrogen bond is observed. A similar arrangement is obtained with 4-pyridyl,[15] imidazolium[18] or pyrazolyl[9] substituted oxotetrazanes. In **1b** and **2b**, an intramolecular hydrogen bond, that is observed in other derivatives when the substituent is in pseudo-equatorial position (**1c**, **1e**, **1f**, **2c**, **2f**), would be only very weak since the geometry of the five-membered imidazole ring would lengthen the distances between the hydrogen atoms of the tetrazane ring and the nitrogen atom of the imidazole. The absence of intramolecular hydrogen bonds may also be due to the intermolecular hydrogen bonding. Such a situation has recently been described in imidazole-substituted urea.[19] In the present case, this argument is reinforced by the fact that due to the sp^3 hybridization of C2 (Scheme 1), we are not in a situation where intramolecular hydrogen bonding is the most favorable according to the systematic survey of Cambridge Structural Database (CSD) performed by Bilton *et al.*[20]

In the absence of an intramolecular hydrogen bond, the preference for the pseudo-axial conformation can be tentatively explained by an electronic effect through hyperconjugative interaction. Such a kind of interaction is proposed as an important factor in the conformational equilibria of 3,5-disubstituted piperidones or cyclohexyl esters.[21–23] In contrast with the intramolecular interactions, the intermolecular interactions are strongly dependent on the nature of the heteroatom borne by the tetrazane ring. A detailed analysis and comparison of the two families of derivatives are thus worthwhile. It can be performed throughout the series except for the pyrimidine-substituted derivatives because only the structure of **1e** has been solved. All the thioxo derivatives

Table 4 Parameters relating to C═S···H bonds

	H-Bond	*d*(C–S)/Å	*d*(S···H)/Å	α/°
1b	C═S···HN1	1.724(2)	2.66	149
	C═S···HN4		2.64	150
1c	C═S···HN1	1.705(1)	2.68	161
1e	C═S···HN1	1.712(2)	2.81	145
	C═S···HN4		2.77	146
1f	C1═S1···HN9	1.717(3)	2.83	151
1g	C═S···HN1	1.715(2)	2.73	154
	C═S···HN4		2.48	154

exhibit intermolecular hydrogen bonds involving the C═S function and NH groups. Allen *et al.* accurately analyzed hydrogen bonding at sulfur acceptors in various systems.[24,25] In Table 4, we adopt the same parameters, *d*(CS), the C═S bond length, *d*(S···H), the S···H distance and α, the S···H–N valence angle to describe these interactions in the **1b–g** series. For comparison, Table 5 gathers the parameters for the oxo-derivatives related to hydrogen bond involving the carbonyl function, when it exists.

The *d*(C–S) values are ranging from 1.705(1) to 1.724(2) Å. This falls into the 1.65–1.72 Å range for seven compounds including the N–N–C(S)–N–N motif found in the CSD though such a low number do not allow any statistical treatment. These values are relatively high compared to the 1.61 Å bond length proposed for a 100% double-bond character. The lengthening of this bond is indeed associated with an increase of the electronic delocalisation.[24] Because of the lower electronegativity of S compared to O, it is well known that C═S bond is less polar. It is thus more sensitive to electronic effects and its length range is broader than that of the C═O bond. Compared to the result of the systematic statistical data analysis performed by Allen *et al.* (Fig. 3 in ref. 24), for both the oxygen and the sulfur derivatives, we observe rather long C═X bond lengths though the C–N distances are also in the medium to long range. This result can be tentatively related to the influence of the lone pairs of the N2 and N3 nitrogen atoms on the electronic delocalisation.

The *d*(S···H) range (2.48–2.83 Å) in our compounds is also in good agreement with the reported values. The longest ones observed for **1e** (2.81 and 2.77 Å) and **1f** (2.83 Å) are still shorter than the sum of van der Waals radii (2.90 Å). The α values are between 145 and 161° which are in the 130–180° range reported by Allen *et al.*[24] In contrast to the oxo derivatives, the electronic delocalisation revealed by the increase of the C═S bond length is indeed the key element for the sulfur to act as a hydrogen-bond acceptor. In the 1.70–1.72 Å range, C═S is involved in hydrogen bonding in more than 70% of the encountered cases.[24]

Allen *et al.* also mentions that the X···H–N valence angle ranges are similar for X = S or O and, when the hydrogen

Table 5 Parameters relating to C═O···H bonds

	H-Bond	*d*(C═O)/Å	*d*(O···H)/Å	α/°
2b	C═O···HN5	1.243(3)	2.03	175
2f	C═O···HN4	1.245(2)	2.55	142
2g	C═O···HN1	1.252(3)	2.16	145
	C═O···HN4		2.20	151

bonds are present, our observations are in accord with this statement.

The crystal packing of thioxo and oxo compounds bearing the imidazole moiety are noticeably different. In **1b**, homomeric associations are observed.[19] This segregation of imidazole–imidazole and tetrazane–tetrazane interactions leads to the formation of a 2D hydrogen-bonded architecture (Fig. 2). In **2b**, the oxygen atom is hydrogen bonded to the NH group of the imidazole substituent (Fig. 2). The O···H–N arrangement is nearly linear (175°) which expresses a strong hydrogen bond as also demonstrated by the short *d*(O···H) value (2.03 Å). This heteromeric association governs the formation of helices along the *c*-axis which are interconnected by hydrogen bonds in the *ab* plane. The comparison of the crystal packing of the pyridine derivatives **1c** and **2c** (Fig. 4) is more surprising. First, no π stacking is observed in **1c** while the combination of π stacking and hydrogen bonding between one NH function of the tetrazane ring and the nitrogen atom of the pyridine of a neighboring molecule in **2c** lead to the formation of mixed supramolecular chains which are similar to those encountered in (6-methyl-2-pyridyl)oxotetrazane.[15] Moreover, whereas an intermolecular hydrogen bond involving the C═S group is observed in **1c**, there is no such interaction involving the carbonyl function in the corresponding oxo derivative **2c**. Such a marked discrepancy is not observed in all the cases. Indeed, both quinolyl substituted tetrazane structures (**1f** and **2f**) are characterized by weak intermolecular hydrogen bonds. In both compounds, these interactions are combined with π–π interactions to give rise to mixed supramolecular extended structures. Nevertheless, in **1f**, the dimensionality of this supramolecular arrangement is two dimensional while it is unidimensional in **2f**. The hydroxyphenyl derivatives (**1g** and **2g**) present a very similar structural arrangement constituted of hydrogen bonding along the *a*-axis. For two neighboring rows, these chains run in opposite directions for **1g** whereas they run in the same direction for **2g**.

Comparison of the hydrogen bonding in these derivatives with the compounds found in the CSD that present the N–N–C(S)–N–N motif can be made. There are seven such derivatives and, for only three of them, the oxygenated analogues have also been described. One pair of derivatives (SIVNAM, SIVMUF) does not present any hydrogen bonding at all because of the absence of hydrogen-donating groups. In the second one (DPCBHZ, DPTCBZ), the hydrogen atoms have not been resolved for the sulfur containing derivative. The third pair is constituted of (thio)carbohydrazide derivatives[26,27] and allows comparison. Hydrogen-bonding features are present in both compounds but, as observed in the case of **1b** and **2b**, they are different. The shorter hydrogen bonds are 2.153 Å (C═O···HN; O···HN angle is 154.4°) and 2.492 Å (C═S···HN; S···HN angle is 157.3°) in the oxygenated (CBOHAZ)[27] and the sulfurated (THCHYD)[26] derivatives, respectively. A scrutiny of the hydrogen-bonding in these compounds within the general framework set by a recent study that compares hydrogen bonding to C═O and C═S acceptors[25] is worthwhile. By combining a statistical treatment of the parameters of hydrogen bonds implying C═X (X = O, S) with intermolecular perturbation theory (IMPT) calculations, the authors demonstrate that, though the difference is reduced upon increased electronic delocalisation, C═O is a better hydrogen-bond acceptor than C═S in any case. Interestingly, the O···HN distance in carbohydrazide[27] is slightly higher than the calculated value found for *N*,*N*′-dimethylurea (1.9 Å) while the S···HN distance in thiocarbohydrazide[26] is slightly shorter than the value calculated for *N*,*N*′-dimethylthiourea (2.6 Å).[25] This statement confirms that the terminal nitrogen atoms of the N–N–C(X)–N–N (X = O, S) motif modulates the hydrogen-bond accepting capability of the X atom in favor of the sulfur atom. Given the moderate energy of hydrogen bonds, they are relatively sensitive to other geometrical and electronic features. In the series of compounds presented here, through increased stiffness, the ring closure of the tetrazane derivatives might reinforce the delocalisation effect mentioned above. Moreover, the steric hindrance brought about by the two methyl groups bonded to N2 and N3 can noticeably reduce the hydrogen-bond accepting ability of the neighboring C═X (X = O, S) function. Due to a reduction of the C═X distance that can reach 0.5 Å when going from sulfur to oxygen, this hindrance is more acute in the latter case. In borderline cases, this phenomenon can preclude the formation of hydrogen bonds for the oxygenated derivatives while it still can form for the corresponding sulfurated compound as observed for **1c** and **2c**.

Conclusion

A series of 1,5-dimethyl-3-R-6-thioxo-1,2,4,5-tetrazanes in which R is a potential coordinative entity have been prepared. Generally, we noticed better yield for the synthesis of the analogous oxo derivatives. The crystal structures of both families of compounds have been described. The conformation of the molecules is fully determined by the nature of the R substituent and independent on X = O or S. It is actually driven by the ability to form intramolecular hydrogen bonds between R and the tetrazane moiety. In the sole example where such interaction is not present, the conformation could be determined by a hyperconjugative effect. The intermolecular interactions (hydrogen bonds, π stacking) observed in these two series of compounds depend both on the R substituent and on the nature of the X heteroatom leading to the formation of pure hydrogen-bonded as well as mixed hydrogen-bonded/π-stacked supramolecular structures whose dimensionality varies from 0 to 2. Actually for a given substituent, the packing is always different for the sulfurated and the oxygenated derivatives, the differences ranging from subtle for the hydroxyphenyl derivatives to striking for the pyridine derivatives. In the latter case, the presence of hydrogen bonds involving the C═S group, whereas C═O is not implied in intermolecular hydrogen bonding in the oxygenated analogue, is surprising though not unexplainable given the combination of electronic effects associated with the tetrazane heterocycle and of the steric hindrance brought about by its two methyl substituents.

By exploiting the versatility of the tetrazane chemistry, it will be possible to gather new crystal packing observations on such systems and by using crystal analysis combined with *ab initio* calculation to go towards reliable predicting rules.

This would allow to use these molecules for crystal engineering as has been done for a while in the urea/thiourea family.[3] Moreover, the ability of such compounds to coordinate metal ions, either as tetrazanes[10–11,28–29] or as verdazyls,[13,30–32] the oxidized form of tetrazane, appears as a valuable way to modulate and enrich the intermolecular interactions.

Experimental

General

(1*H*-Imidazole)-2-carbaldehyde, 2-pyridinecarbaldehyde, glyoxylic acid, 8-quinolinecarbaldehyde and salicylaldehyde were used as purchased. 4,6-Dimethyl-2-pyrimidinecarbaldehyde was prepared following the route developed by Barr *et al.*[7] 2,4-Dimethylthiocarbonohydrazide **1a** and 2,4-dimethylcarbonohydrazide **2a** were prepared according to the literature.[4] The synthesis and characterization of compounds **2b–e** and **2g** have already been reported.[4,7,12,15]

The ^{1}H and ^{13}C{^{1}H} NMR spectra were recorded using a Bruker Avance 400 NMR spectrometer at 400 and 101 MHz, respectively; chemical shifts δ in ppm with respect to $SiMe_4$, J in Hz. Infrared spectra were recorded from KBr discs on a Bio-Rad FTIR spectrometer FTS 165; ν in cm^{-1}. Elemental analyses were performed at Service Central d'Analyses du CNRS in Vernaison (France).

Synthesis of compounds

All the reactions occurred in refluxing methanol, except that for the synthesis of the 6-(2′-hydroxyphenyl) derivatives **1g** and **2g** which were carried on at room temperature. The synthesis of **1b** is fully described as a representative example.

1,5-Dimethyl-3-(2′-imidazolyl)-6-thioxo-1,2,4,5-tetrazane 1b

1a (1.653 g, 12.3 mmol) was dissolved in 140 mL of methanol. The solution was heated to 60 °C before a suspension of 1*H*-imidazole-2-carbaldehyde (1.184 g, 12.3 mmol) in 240 mL of methanol was added dropwise. 30 min after the end of the addition, the reaction mixture was suspension-free. The solution was then refluxed overnight. Finally, the solvent was removed by evaporation under reduced pressure to give a light yellow solid. Colorless crystals (1.508 g, 58%) suitable for X-ray diffraction were obtained by recrystallization from a 2 : 1 ethyl acetate–methanol mixture.

^{1}H NMR (400 MHz, d^{6}-DMSO, ppm): 7.01 (br s, 2H, CH_{im}), 5.78 (d, 2H, J = 10 Hz, NH), 4.96 (t, 1H, J = 10 Hz, C_2H), 3.43 (s, 6H, CH_3). ^{13}C NMR (101 MHz, d^{6}-DMSO, ppm): 174.3 (C═S), 143.3, 129.2, 118.6, 65.4 (C2), 45.3. IR (cm^{-1}): ν_{max} 3167 (m), 3153 (NH, m), 2930 (CH, m), 1508 (m), 1420 (s), 1373 (s), 1088 (s), 1060 (s), 765 (s), 462 (s). Elemental analysis. Found: C, 39.38; H, 5.84; N, 39.09; S, 14.64%. $C_7H_{12}N_6S$ requires C, 39.62; H, 5.66; N, 39.62; S, 15.09%.

1,5-Dimethyl-3-(2′-pyridyl)-6-thioxo-1,2,4,5-tetrazane 1c

As **1b**. Colorless crystals (M = 223 g mol^{-1}, 44%) were obtained.

^{1}H NMR (400 MHz, d^{6}-DMSO, ppm): 8.58 (d, 1H, J = 4.8 Hz, H_{Pyr}), 7.87 (t, 1H, J = 7.7 Hz, H_{Pyr}), 7.56 (d, 1H, J = 7.7 Hz, H_{Pyr}), 7.42 (dd, 1H, J = 7.7 and 4.8 Hz, H_{Pyr}), 5.80 (d, 2H, J = 10.4 Hz, NH), 4.96 (t, 1H, J = 10.4 Hz, C_2H), 3.45 (s, 6H, CH_3). ^{13}C NMR (101 MHz, $CDCl_3$, ppm): 171.9 (C═S), 151.6, 148.4, 135.9, 123.0, 122.2, 67.4 (C2), 43.2. IR (cm^{-1}): ν_{max} 3174 (NH, m), 2932 (CH, w), 1596 (m), 1475 (s), 1436 (s), 1326 (s), 1292 (s), 1085 (s), 935 (s), 773 (s), 483 (s). Elemental analysis. Found: C, 48.55; H, 6.03; N, 31.28; S, 13.92%. $C_9H_{13}N_5S$ requires C, 48.43; H, 5.83; N, 31.39; S, 14.35%.

1,5-Dimethyl-3-carboxy-6-thioxo-1,2,4,5-tetrazane 1d

As **1b**. Recrystallization of the residue from a 5 : 1 ethyl acetate–methanol mixture afforded a white crystalline powder (M = 190 g mol^{-1}, 75%).

^{1}H NMR (400 MHz, d^{6}-DMSO, ppm): 5.79 (br s, 2H, NH), 4.48 (s, 1H, CH), 3.39 (s, 6H, CH_3). ^{13}C NMR (101 MHz, d^{6}-DMSO, ppm): 173.3 (C═S), 168.1 (C═O), 66.8, 43.8.

IR (cm^{-1}): ν_{max} 3508 (OH, m), 3163 (m), 3128 (NH, m), 2936 (CH, m), 2463 (m), 1717 (CO), 1508 (m), 1475 (m), 1426 (m), 1351 (m), 1246 (s), 1081 (s), 962 (s), 874 (s), 759 (m), 704 (m), 481 (s). Elemental analysis. Found: C, 28.82; H, 5.88; N, 26.81; S, 15.03%. $C_5H_{10}N_4SO_2{\cdot}H_2O$ requires C, 28.85; H, 5.77; N, 26.92; S, 15.38%.

1,5-Dimethyl-3-(4′,6′-dimethylpyrimidyl)-6-thioxo-1,2,4,5-tetrazane 1e

As **1b**. Recrystallization of the residue from ethyl acetate afforded colorless crystals (M = 252 g mol^{-1}, 71%).

^{1}H NMR (400 MHz, $CDCl_3$, ppm): 7.07 (s, 1H, H_{aro}), 4.97 (s, 1H, C_2H), 4.70 (br s, 2H, NH), 3.66 (s, 6H, NCH_3), 2.52 (s, 6H, CH_3) ppm. ^{13}C NMR (101 MHz, $CDCl_3$, ppm): 175.0 (C═S), 169.1, 162.8, 121.6, 71.3 (C2), 45.7 (NCH_3), 24.9 (CH_3). IR (cm^{-1}): ν_{max} 3169 (m), 3150 (NH, m), 2923 (CH, w), 1597 (s), 1542 (m), 1487 (s), 1437 (s), 1332 (s), 1287 (s), 1080 (s), 948 (s), 866 (s), 542 (m), 491 (m). Elemental analysis. Found: C, 47.70; H, 6.69; N, 33.40; S, 12.51%. $C_{10}H_{16}N_6S$ requires C, 47.62; H, 6.35; N, 33.33; S, 12.70%.

1,5-Dimethyl-3-(8′-quinolyl)-6-thioxo-1,2,4,5-tetrazane 1f

As **1b**. Recrystallization of the residue from a 3 : 1 ethyl acetate–methanol mixture afforded light-brown crystals (M = 273 g mol^{-1}, 51%).

^{1}H NMR (400 MHz, $CDCl_3$, ppm): 8.86 (dd, 1H, J = 4.3 and 1.8 Hz, H_{aro}), 8.26 (dd, 1H, J = 8.3 and 1.8 Hz, H_{aro}), 7.88 (dd, 1H, J = 8.3 and 1.4 Hz), 7.79 (dd, 1H, J = 7.0 and 1.4 Hz), 7.59 (dd, 1H, J = 8.3 and 7.1 Hz), 7.50 (dd, 1H, J = 8.3 and 4.3 Hz), 6.51 (d, 2H, J = 11.5 Hz, NH), 5.17 (t, 1H, J = 11.5 Hz, C_2H), 3.71 (s, 6H, CH_3). ^{13}C NMR (101 MHz, $CDCl_3$, ppm): 174.3 (C═S), 151.1, 147.3, 138.5, 132.4, 130.5, 130.1, 128.0, 122.8, 74.8 (C2), 45.8. IR (cm^{-1}): ν_{max} 3208 (m), 3172 (NH, m), 2918 (CH, m), 1596 (m), 1499 (s), 1464 (s), 1428 (s), 1373 (s), 1090 (s), 939 (s), 823 (s), 790 (s). Elemental analysis. Found: C, 57.04; H, 5.65; N, 25.53; S, 11.42%. $C_{13}H_{15}N_5S$ requires C, 57.14; H, 5.49; N, 25.64; S, 11.72%.

1,5-Dimethyl-3-(2′-hydroxyphenyl)-6-thioxo-1,2,4,5-tetrazane 1g

The reaction of **1a** (1.092 g, 8.1 mmol) with 0.7 mL of salicylaldehyde (ρ = 1.16 g mL, 6.8 mmol) in 160 mL of methanol occurred at room temperature overnight. A mixture

of the target molecule (91%, estimated by ^{1}H NMR) and diimine (9%) was obtained. The crude solid was washed with a few mL of chloroform and the product was isolated as a white powder (0.971 g, 60%).

^{1}H NMR (400 MHz, d^6-DMSO, ppm): 9.82 (s, 1H, OH), 7.27 (dd, 1H, J = 7.5 and 1.5 Hz, H_{aro}), 7.16 (m, 1H, H_{aro}), 6.85 (m, 2H, H_{arom}), 5.85 (d, 2H, J = 10.3 Hz, NH), 5.04 (t, 1H, J = 10.3 Hz, C_2H), 3.43 (s, 6H, CH_3). ^{13}C NMR (101 MHz, d^6-DMSO, ppm): 173.8 (C=S), 156.4, 131.2, 129.2, 123.2, 120.7, 117.1, 66.4 (C2), 45.2. IR (cm^{-1}): ν_{max} 3140 (NH, m), 2979 (w), 2923 (CH, w), 1617 (m), 1588 (m), 1521 (s), 1474 (s), 1364 (s), 1288 (s), 1237 (s), 1095 (s), 1059 (s), 959 (s), 834 (s), 754 (s), 473 (s). Elemental analysis. Found: C, 50.32; H, 5.96; N, 23.54; S, 13.66%. $C_{10}H_{14}N_4SO$ requires C, 50.42; H, 5.88; N, 23.53; S, 13.45%.

1,5-Dimethyl-3-(8′-quinolyl)-6-oxo-1,2,4,5-tetrazane 2f

2a (0.376 g, 3.2 mmol) was dissolved in 100 mL of methanol. The solution was heated to 60 °C before a solution of 8-quinolinecarbaldehyde (0.475 g, 3.0 mmol) in 150 mL of methanol was added dropwise. The solution was then refluxed for 2 h. Finally, the solvent was removed by evaporation under reduced pressure to give a pale yellow solid. Recrystallization of the residue from a 5 : 1 ethyl acetate–methanol mixture afforded pale orange crystals (0.772 g, 67%).

^{1}H NMR (400 MHz, d^6-DMSO, ppm): 8.91 (dd, 1H, J = 4.2 and 1.8 Hz, H_{aro}), 8.37 (dd, 1H, J = 8.7 and 1.8 Hz, H_{aro}), 7.94 (dd, 1H, J = 8.1 and 1.5 Hz, H_{aro}), 7.83 (dd, 1H, J = 6.9 and 1.5 Hz, H_{aro}), 7.53–7.58 (m, 2H, H_{arom}), 6.22 (d, 2H, J = 11.4 Hz, NH), 5.59 (t, 1H, J = 11.4 Hz, C_2–H), 3.00 (s, 6H, CH_3). ^{13}C NMR (101 MHz, d^6-DMSO, ppm): 156.1 (C=O), 151.8, 146.6, 138.5, 135.0, 130.3, 130.1, 129.6, 127.9, 123.3, 70.0 (C2), 39.2 (CH_3). IR (cm^{-1}): 3230 (m), 3037 (m), 2916 (CH, m), 1628 (CO, s), 1594 (m), 1483 (m), 1434 (s), 1386 (s), 954 (s), 890 (s), 829 (s), 791 (s), 521 (s). Elemental analysis. Found: C, 60.59; H, 5.90; N, 27.17% $C_{13}H_{15}N_5O$ requires C, 60.70; H, 5.84; N, 27.23%.

1,5-Dimethyl-3-(2′-hydroxyphenyl)-6-oxo-1,2,4,5-tetrazane 2g

The reaction of **2a** (2.486 g, 21.2 mmol) with 1.8 mL of salicylaldehyde (17.1 mmol) in 250 mL of methanol occurred at room temperature overnight. The solvent was removed by evaporation under reduced pressure. The crude solid was washed with ethyl acetate (2 × 10 mL) and the product was isolated as a white powder. Recrystallization from a 1 : 1 ethyl acetate–methanol mixture afforded colorless crystals (2.600 g, 69%).

^{1}H NMR (400 MHz, d^6-DMSO, ppm): 9.85 (s, 1H, OH), 7–8 (m, 4H, H_{aro}), 7.16 (m, 1H, H_{aro}), 5.72 (d, 2H, J = 9.9 Hz, NH), 5.02 (t, 1H, J = 9.9 Hz, N–CH), 2.96 (s, 6H, CH_3). ^{13}C NMR (101 MHz, d^6-DMSO, ppm): 156.6 (C=O), 155.8, 130.9, 129.2, 123.3, 120.6, 117.2, 67.6 (C2), 39.0 (CH_3). IR (cm^{-1}): ν_{max} 3232 (m), 2982 (CH, m), 2878 (w), 1599 (s), 1579 (s), 1480 (s), 1222 (s), 980 (s), 838 (m), 754 (s), 521 (s). Elemental analysis. Found: C, 53.88; H, 6.16; N, 25.17%. $C_{10}H_{14}N_4O_2$ requires C, 54.04; H, 6.35; N, 25.21%.

X-Ray crystallography

A single crystal of each compound was selected, mounted onto a glass fiber, and transferred in a cold nitrogen gas stream. Intensity data were collected with a Bruker-Nonius Kappa-CCD with graphite-monochromated Mo-Kα radiation (0,71073 Å). Unit-cell parameters determination, data collection strategy and integration were carried out with the Nonius EVAL-14 suite of programs.[33] Multi-scan absorption correction was applied.[34] The structure was solved by direct methods using the SIR92 program[35] and refined anisotropically by full-matrix least-squares methods using the SHELXL-97 software package.[36] Hydrogen atoms involved in hydrogen bonding were located from Fourier difference map and restrained to their position.

Acknowledgements

This work was developed within the framework of the ANR project 'fdp magnets' in particular through the post-doctoral grant of Olivier Oms. It was also supported by the UPMC, Univ Paris 06 and CNRS. Lucie Norel acknowledges the Ministère de l'Enseignement Supérieur et de la Recherche (MESR) for her PhD grant.

References

1 G. R. Desiraju, *Angew. Chem., Int. Ed.*, 2007, **46**, 8342.
2 J. D. West, *Chem. Commun.*, 2005, 5830.
3 R. Custelcean, *Chem. Commun.*, 2008, 295.
4 F. A. Neugebauer, H. Fischer, R. Siegel and C. Krieger, *Chem. Ber.*, 1983, **116**, 3461.
5 F. A. Neugebauer, H. Fischer and R. Siegel, *Chem. Ber.*, 1988, **121**, 815.
6 F. A. Neugebauer, H. Fischer and C. Krieger, *J. Chem. Soc., Perkin Trans. 2*, 1993, 535.
7 C. L. Barr, P. A. Chase, R. G. Hicks, M. T. Lemaire and C. L. Stevens, *J. Org. Chem.*, 1999, **64**, 8893.
8 R. M. Fico Jr, M. F. Hay, S. Reese, S. Hammond, E. Lambert and M. A. Fox, *J. Org. Chem.*, 1999, **64**, 9386.
9 J.-Z. Wu, E. Bouwman, J. Reedijk, A. M. Mills and A. L. Spek, *Inorg. Chim. Acta*, 2003, **351**, 326.
10 T. M. Barclay, R. G. Hicks, M. T. Lemaire, L. K. Thompson and Z. Xu, *Chem. Commun.*, 2002, 1688.
11 M. T. Lemaire, T. M Barclay, L. K. Thompson and R. G. Hicks, *Inorg. Chim. Acta*, 2006, **359**, 2616.
12 L. Norel, F. Pointillart, C. Train, L.-M. Chamoreau, K. Boubekeur, Y. Journaux, A. Brieger and D. J. R. Brook, *Inorg. Chem.*, 2008, **47**, 2396.
13 B. D. Koivisto and R. G. Hicks, *Coord. Chem. Rev.*, 2005, **249**, 2612.
14 C. Train, L. Norel and M. Baumgarten, *Coord. Chem. Rev.*, 2009, DOI: 10.1016/j.ccr.2008.10.004.
15 M. J. Plater, J. P. Sinclair, S. Kemp, T. Gelbrich, M. B. Hursthouse and C. J. Gomez-Garcia, *J. Chem. Res.*, 2006, **8**, 515.
16 N. Yoshioka, M. Irisawa, Y. Mochizuki, T. Aoki and H. Inoue, *Mol. Cryst. Liq. Cryst.*, 1997, **306**, 403.
17 C. Janiak, *J. Chem. Soc., Dalton Trans.*, 2000, 3885.
18 A. M. Mills, J.-Z. Wu, E. Bowman, J. Reedijk and A. L. Spek, *Acta Crystallogr., Sect. E*, 2004, **60**, 2482.
19 Y.-M. Legrand, M. Michau, A. van der Lee and M. Barboiu, *CrystEngComm*, 2008, **10**, 490.
20 C. Bilton, F. H. Allen, G. P. Shields and J. A. K. Howard, *Acta Crystallogr., Sect. B*, 2000, **56**, 849.
21 E. Kleinpeter, *Adv. Heterocycl. Chem.*, 2004, **86**, 41.
22 E. Kleinpeter, F. Taddei and P. Wacker, *Chem.–Eur. J.*, 2003, **9**, 1360.
23 L. Yuan, B. G. Sumpter, K. A. Abboud and R. K. Castellano, *New J. Chem.*, 2008, **32**, 1924.

24 F. H. Allen, C. M. Bird, R. S. Rowland and P. R. Raithby, *Acta Crystallogr., Sect. B*, 1997, **53**, 680.
25 P. A. Wood, E. Pidcock and F. H. Allen, *Acta Crystallogr., Sect. B*, 2008, **64**, 491.
26 A. Braibanti, A. Tiripicchio and M. Tiripicchio Camellini, *Acta Crystallogr.,Sect. B*, 1969, **25**, 2286.
27 P. Domiano, M. A. Pellinghelli and A. Tiripicchio, *Acta Crystallogr., Sect. B*, 1972, **28**, 2495.
28 D. J. R. Brook, S. Fornell, J. E. Stevens, B. Noll, T. H. Koch and W. Eisfeld, *Inorg. Chem.*, 2000, **39**, 562.
29 F. Pointillart, C. Train, P. Herson, J. Marrot and M. Verdaguer, *New J. Chem.*, 2007, **31**, 1001.
30 R. G. Hicks, M. T. Lemaire, L. K. Thompson and T. M. Barclay, *J. Am. Chem. Soc.*, 2000, **122**, 8077.
31 J. B. Gilroy, B. D. Koivisto, R. McDonald, M. J. Ferguson and R. G. Hicks, *J. Mater. Chem.*, 2006, **16**, 2618.
32 L. Norel, L.-M. Chamoreau, Y. Journaux, O. Oms, G. Chastanet and C. Train, *Chem. Commun.*, 2009, 2381.
33 A. J. M. Duisenberg, L. M. J. Kroon-Batenburg and A. M. M. Schreurs, *J. Appl. Crystallogr.*, 2003, **36**, 220.
34 R. H. Blessing, *Acta Crystallogr., Sect. A*, 1995, **51**, 33.
35 A. Altomare, G. Cascarano, C. Giacovazzo and A. Guagliardi, *J. Appl. Crystallogr.*, 1993, **26**, 343–350.
36 G. M. Sheldrick, *Acta Crystallogr., Sect. A*, 2008, **64**, 112–122.

